Nrf2 activation protects against solar-simulated ultraviolet radiation in mice and humans

Elena V. Knatko,[1] Sally H. Ibbotson,[2] Ying Zhang,[1] Maureen Higgins,[1] Jed W. Fahey,[3,4] Paul Talalay,[3] Robert S. Dawe,[2] James Ferguson,[2] Jeffrey T.-J. Huang,[1] Rosemary Clarke,[5] Suqing Zheng,[6] Akira Saito,[6] Sukirti Kalra,[1] Andrea L. Benedict,[3] Tadashi Honda,[6,7] Charlotte M. Proby,[1,2] and Albena T. Dinkova-Kostova[1,3,*]

[1]*Jacqui Wood Cancer Centre, Division of Cancer Research, Medical Research Institute, University of Dundee, Dundee, DD1 9SY, Scotland, UK*

[2]*Photobiology Unit, Ninewells Hospital and Medical School, University of Dundee, Dundee DD1 9SY, Scotland, UK*

[3]*Lewis B. and Dorothy Cullman Cancer Chemoprotection Center, Department of Pharmacology and Molecular Sciences, Johns Hopkins University School of Medicine, Baltimore, MD 21205, USA*

[4]*Center for Human Nutrition, Department of International Health, Johns Hopkins University Bloomberg School of Public Health, Baltimore, MD 21205, USA*

[5]*Division of Cell Signaling and Immunology, College of Life Sciences, University of Dundee, Dundee DD1 5EH, Scotland, UK*

[6]*Institute of Chemical Biology and Drug Discovery, Stony Brook University, Stony Brook, New York 11794, USA*

[7]*Department of Chemistry, Stony Brook University, Stony Brook, New York 11794, USA*

*To whom correspondence should be addressed: Albena T. Dinkova-Kostova, Division of Cancer Research, Medical Research Institute, James Arrott Drive, Ninewells Hospital and Medical School, Dundee DD1 9SY, UK. Tel: 44-1382-383386; Email: a.dinkovakostova@dundee.ac.uk

Running Title: Nrf2 activation protects against UV radiation

Disclosure of Potential Conflicts of Interest: None of the authors have any potential conflict of interest to disclose.

1

2

Abstract

The transcription factor Nrf2 determines the ability to adapt and survive under conditions of electrophilic, oxidative and inflammatory stress by regulating the expression of elaborate networks comprising nearly 500 genes encoding proteins with versatile cytoprotective functions. In mice, disruption of Nrf2 increases susceptibility to carcinogens and accelerates disease pathogenesis. Paradoxically, Nrf2 is upregulated in established human tumors, but whether this upregulation drives carcinogenesis is not known. Here we show that the incidence, multiplicity and burden of solar-simulated UV radiation-mediated cutaneous tumors that form in SKH-1 hairless mice in which Nrf2 is genetically constitutively activated, are lower than those that arise in their wild-type counterparts. Pharmacological Nrf2 activation by topical bi-weekly applications of small (40 nmol) quantities of the potent bis(cyano enone) inducer TBE-31 has a similar protective effect against solar-simulated UV radiation in animals receiving long-term treatment with the immunosuppressive agent azathioprine. Genetic or pharmacological Nrf2 activation lowers the expression of the pro-inflammatory factors interleukin (IL)-6 and IL-1β, and cyclooxygenase (COX)-2 after acute exposure of mice to UV radiation. In healthy human subjects, topical applications of extracts delivering the Nrf2 activator sulforaphane, reduced the degree of solar-simulated UV radiation-induced skin erythema, a quantifiable surrogate end-point for cutaneous damage and skin cancer risk. Collectively, these data show that Nrf2 is not a driver for tumorigenesis even upon exposure to a very potent and complete carcinogen, and strongly suggest that the frequent activation of Nrf2 in established human tumors is a marker of metabolic adaptation.

3

Introduction

The cap'n'collar (CNC) basic-region leucine zipper (bZIP) transcription factor NF-E2 p45-related factor 2 (Nrf2, also called Nfe2l2) orchestrates a transcriptional program comprising nearly 500 genes encoding cytoprotective proteins, which allow adaptation and survival under conditions of electrophilic and oxidative stress (1-3). The diverse functions of the transcriptional targets of Nrf2 include antioxidant and drug-metabolizing enzymes, as well as proteins that participate in glucose, lipid, and nucleotide metabolism, placing this transcription factor at the interface between cellular redox and intermediary metabolism (4). Under homeostatic conditions, Nrf2 is mainly regulated by Kelch-like ECH-associated protein 1 (Keap1), a Cullin (Cul)-3/Rbx1 ubiquitin ligase substrate adaptor protein that mediates continuous ubiquitination and proteasomal degradation of the transcription factor (5-7). In addition to being a repressor for Nrf2, Keap1 is also the cellular sensor for a wide array of sulfhydryl-reactive small molecules (termed inducers) that chemically modify the sensor cysteines of Keap1, leading to loss of repressor function, Nrf2 stabilization, and upregulation of downstream target gene expression (8, 9). A large body of experimental evidence has demonstrated that the absence of Nrf2 increases the sensitivity to numerous carcinogens and accelerates disease progression. Conversely, Nrf2 activation by pharmacological agents protects against cancer in various animal models. Paradoxically however, Nrf2 is frequently activated in human tumors and contributes to resistance to chemotherapy and radiation therapy (10, 11).

Non-melanoma skin cancers are the most common human malignancies, with more than two million new cases diagnosed globally each year (12). Furthermore, cutaneous squamous cell carcinomas (cSCC) are among the most highly mutated human cancers, carrying one mutation per ~30,000 bp of coding sequence (13). The risk for cSCC is particularly high and its management is especially problematic in specific high-risk groups,

4

such as solid organ transplant recipients receiving life-long immunosuppressive therapies, for whom skin cancer is a major cause of morbidity and mortality (14). Solar ultraviolet (UV) radiation, the most abundant carcinogen in our environment, is the main factor in the etiology of cSCC, both in the general and the immunosuppressed populations, causing generation of reactive oxygen species (ROS), direct and indirect (oxidative) DNA damage, inflammation, and immunosuppression. Most of these damaging processes are counteracted by the endogenous cytoprotective mechanisms that are regulated by Nrf2. It has been previously shown that small molecule activators of Nrf2 protect against UVA- or UVB radiation-induced damage in cells and *in vivo* (15). In female C57BL/6 and CD-1 mice, the Nrf2 activator sulforaphane protects against oncogenic H-Ras(Q61L)-driven papilloma formation in the 7,12-dimethylbenz[a]anthracene/12-*O*-tetradecanoylphorbol-13-acetate (DMBA/TPA) model (16, 17). Topical or dietary administration of sulforaphane-rich broccoli sprout extracts is also protective against UVB radiation-mediated skin carcinogenesis in female SKH-1 hairless mice (18, 19). However, it is unclear whether this protection extends to solar UV radiation, which comprises both UVA and UVB wavelengths and is much more relevant to human exposure to sunlight than either UVA or UVB individually. Furthermore, it is not known whether pharmacological activation of Nrf2 protects against the development of cSCC caused by solar UV radiation under conditions of life-long immunosuppressive therapy. In addition, given that Nrf2 is often activated in established tumors, a critical question arises whether constitutive Nrf2 activation could be a driver for tumor development.

To address these questions, we generated SKH-1 hairless mice in which Nrf2 is either disrupted or constitutively activated. SKH-1 hairless mice are immunocompetent, but have a defect in the hairless (*Hr*) gene encoding a transcriptional co-repressor, the loss of which renders the animals hairless after completion of the first hair cycle (20). By use of these new mouse models, we found that genetic activation of Nrf2 protects against skin carcinogenesis

5

evoked by solar-simulated UV radiation, indicating that constitutive Nrf2 activation does not drive cutaneous tumor development even upon exposure to a complete (both an initiator and a promoter) carcinogen. We further show that topical twice-weekly applications of small (nanomol) quantities of the potent pharmacological Nrf2 activator TBE-31, a tricyclic bis(cyano enone) (21), greatly reduces the multiplicity and volume of tumors that form after chronic exposure to solar-simulated UV radiation in SKH-1 hairless mice receiving the immunosuppressive agent azathioprine. Additionally, in healthy human subjects, topical application of extracts containing an Nrf2 activator, sulforaphane, reduced the degree of skin erythema following acute exposure to solar-simulated UV radiation.

Materials and Methods

Materials

All chemicals and reagents were obtained from common commercial suppliers and were of the highest purity available. ($\pm$)-TBE-31 was synthesized as described (21, 22). A stable isotope labeled ($\pm$)-[$^{13}C_2^{15}N_2$]-TBE-31 was synthesized in four steps from a previously reported intermediate (22), which is prepared in 11 steps from cyclohexanone, by introduction of two ^{13}C atoms with ethyl [^{13}C]formate and two ^{15}N atoms with hydroxy[^{15}N]amine (23).

Animals and treatments

All animal experiments were performed in accordance with the regulations described in the UK Animals (Scientific Procedures) Act 1986, and were in strict compliance with institutional guidelines. SKH-1 hairless mice were initially obtained from Charles River (Germany), and then bred in our facility with free access to water and food (pelleted RM1 diet from SDS Ltd., Witham, Essex, UK), on a 12-h light/ 12-h dark cycle, 35% humidity.

6

Nrf2-KO and Keap1-KD SKH-1 hairless mice were generated by back-crossing Nrf2-KO

(24) and Keap1-KD (25) C57BL/6 mice onto the SKH-1 hairless genetic background over six

generations. All experimental animals were age-matched and female.

For experiments with azathioprine, the animals were housed in individually ventilated

cages. Azathioprine (Sigma-Aldrich Co, Poole, Dorset, UK), was freshly prepared in 0.05 N

NaOH and diluted at a ratio of 1:500 (v/v) into the drinking water to a final concentration of

61.25 μg/ml, resulting in the animals receiving azathioprine at a dose of 1 mg/kg/day. The

water bottles were changed three times per week and were kept wrapped in aluminium foil to

protect azathioprine from light exposure. TBE-31 was applied topically in 200 μl of 80%

acetone (v/v) over the entire back (dorsal skin) of the mouse. Control mice received 200 μl of

80% acetone (v/v). At the end of each experiment, the animals were euthanized, and blood

was drawn by cardiac puncture and collected in Eppendorf tubes containing 5 μl of 500 mM

EDTA. Plasma was obtained by centrifugation at 25 °C (300 x g for 20 min) and immediately

frozen in liquid N_2. Skin, liver, and kidneys were harvested immediately after blood draw,

frozen in liquid N_2, and stored at – 80 °C until analysis. For TBE-31 pharmacokinetic

experiments, harvested dorsal skin from the site of application was first rinsed in PBS,

blotted on filter paper, and then frozen.

Exposure of mice to solar-simulated UV radiation

The UV lamps (UVA340, Q-Lab, Germany) used to irradiate the animals provide a

near-perfect simulation of sunlight in the critical short wavelength region, from 365 nm to the

solar cutoff of 295 nm, with a peak emission at 340 nm (Fig. S1). The radiant dose was

quantified, at the appropriate distance, with a UVB Daavlin Flex Control Integrating

Dosimeter and further confirmed with an external radiometer (X-96 Irradiance Meter;

Daavlin, Bryan, OH) before and after each irradiation session. An electrical fan was used to

7

avoid excessive heating. For acute radiation experiments, the animals were exposed to UV radiation in groups and euthanized 24- or 72 h after irradiation. Dorsal skin was harvested, immediately frozen in liquid N_2, and stored at -80 °C.

For skin carcinogenesis experiments, the animals were exposed twice a week for 15 weeks on Tuesdays and Fridays to solar-simulated UV radiation (comprised of 2 J/cm^2 UVA and 90 mJ/cm^2 UVB) in clear bedding-free cages. For the study comparing the three genotypes of mice, the animals were randomized in such a way that every cage contained representatives of each genotype. Treatment with TBE-31 (40 nmol per mouse, applied topically in 200 μl of 80% acetone v/v over the entire back of the animal, bi-weekly, on Mondays and Thursdays or 200 μl of 80% acetone vehicle control) and azathioprine (1 mg/kg, daily, *per os*) began two weeks prior to the first exposure to UV radiation and continued throughout the experiment. Tumors (defined as lesions >1 mm in diameter) and body weights were recorded weekly. Tumor volumes ($v = 4\pi r^3/3$) were determined by measuring the height, length, and width, and using the average of the three measurements as the diameter.

Biochemical analyses

Frozen tissue was pulverized into powder under liquid N_2. The powder was weighed and ~30 mg were resuspended in ice-cold buffer [100 mM potassium phosphate, pH 7.4; 100 mM KCl; 0.1 mM ethylenediaminetetraacetic acid (EDTA)], homogenized in an ice bath, and subjected to centrifugation at 4 °C (15,000 x g for 10 min). The enzyme activities of NQO1 with menadione as a substrate (26) and of GST with CDNB as a substrate (27) were determined in supernatant fractions. Protein concentrations were measured by the bicinchoninic acid (BCA) assay (Thermo Scientific).

For western blot analysis of the levels of Keap1, Nrf2, and GCLC, skin powder (~30 mg) was resuspended and homogenized in ice-cold radioimmunoprecipitation assay buffer

8

(50 mM Tris-HCl, pH 7.5; 150 mM NaCl; 1% NP-40; 0.5% sodium deoxycholate; 0.1% sodium dodecyl sulfate; 1 mM EDTA, with added EDTA-free protease inhibitors cocktail, Roche). Proteins were separated by electrophoresis on a 10% sodium dodecyl sulfate–polyacrylamide gel, and then electrophoretically transferred to immobilon-P membrane (Millipore, Watford, Herts., UK). After blocking with 10% non-fat milk at 4°C for 2 h, immunoblotting was performed using the following antibodies: rabbit polyclonal Nrf2 antibody at a dilution of 1:2000, rabbit polyclonal Keap1 antibody at a dilution of 1:2000, or sheep GCLC antibody at a dilution of 1:2500 (all kind gifts from John D. Hayes, University of Dundee) (28). Antibodies against glyceraldehyde-3-phosphate dehydrogenase (GAPDH, Sigma–Aldrich Co., 1:5000 dilution) or β-actin (Sigma–Aldrich Co., 1:10000 dilution) were used as loading controls.

Quantitative real-time PCR

The primers and probes (TaqMan® Gene Expression Assays) used to measure the mRNA levels for Keap1, Nrf1, Nrf3, NQO1, GSTP, GCLC, HMOX-1, IL-6, IL-1β, and COX2 were from Life Technologies. Total RNA was extracted from mouse skin using RNeasy Fibrous Tissue Kit (Qiagen Ltd.). Omniscript RT Kit (Qiagen Ltd.) was then used to reverse-transcribe 500 ng of total RNA into cDNA. Real-time PCR was carried out on Perkin Elmer/Applied Biosystems Prism Model 7700 Sequence Detector instrument. The TaqMan data for the mRNA species were normalized using β-actin (mouse ACTB, 4352933E) as an internal control.

Extract treatment and exposure of healthy human subjects to solar-simulated UV radiation

The human study was approved by the East of Scotland Research Ethics Service and

9

the Institutional Review Board of Johns Hopkins University. Informed consent was obtained

from each participant after the nature and possible consequences of the study were fully

explained. The extracts were prepared and analyzed as described in Supplemental Methods

(26, 29), and dispensed in containers wrapped in aluminium foil that do not state their

contents (marked "L" and "M"). Thus, subjects, assessors and those applying the extracts did

not know which was active and which was placebo. To determine which side (left or right) of

the back is to receive active and which placebo, a random allocation sequence was produced

using blocked computerized random allocation, with allocations for each subject concealed in

an opaque envelope. On days 1-3, after gently cleaning the skin with isopropyl alcohol, the

right or the left half of the mid-upper back skin of each volunteer received, as randomly

allocated, active or placebo extracts (delivering 200 nmol/cm^2 of sulforaphane or

glucoraphanin), respectively, three times, 24 h apart. On day 4, the extract-treated areas were

washed gently with saline followed by isopropyl alcohol in order to remove any residual

surface extract. Then, small areas of the skin (approximately 1 cm^2) within the treated areas

were exposed to a range of doses of ultraviolet and visible light from a monochromator 450W

xenon arc source (at specific wavebands centered on 305, 335, 365, and 400 nm), and solar-

simulated UV radiation from a 150W xenon arc filtered source, the emission spectrum of

which approximates the mid-day summer solar spectrum. The intensity of erythemal

responses at the active- and placebo-treated sites was determined 24 h later – assessing

threshold erythema response (minimal erythema dose), and overall sum of intensity of

erythema. Minimal erythemal dose (MED) was defined as the dose required to give minimal

perceptible redness. It was planned to go onto a study to assess whether or not there might be

changes in human tissue associated with photoprotection only if with at least one of the

wavebands tested in the human study there was a photoprotection factor of ≥ 1.4 and/or a

change of erythema of $\geq$ to 20% detected.

10

Statistical analysis

Values are means ± 1 S.D. or 1 S.E.M., as indicated in the figure legends. The differences between groups were determined by Students t-test or by ANOVA, as indicated in the figure legends. Analyses were performed using either Excel (Microsoft Corp.) or Stata 11.2 (Statacorp, College Station, TX, USA).

Results

Genetic upregulation of Nrf2 protects against inflammation caused by solar-simulated UV radiation

We generated SKH-1 hairless mice in which Nrf2 is either disrupted or constitutively activated by back-crossing Nrf2-knockout (Nrf2-KO) (24) and Keap1-knockdown (Keap1-KD) (25) C57BL/6 mice onto the SKH-1 hairless genetic background over six generations. Keap1-KD mice carry two floxed alleles of the *keap1* gene, which reduces its expression and consequently increases the levels of Nrf2, and thus represent a genetic model for constitutive Nrf2 activation (25). The mRNA and protein levels of Keap1 in samples isolated from skin of Nrf2-KO SKH-1 hairless mice are comparable to those of wild-type (WT) animals; however the mRNA levels of Keap1 are 75% lower, and the protein levels are also reduced by ~60% in their Keap1-KD counterparts (Fig. 1A,B). As expected, Nrf2-KO SKH-1 hairless animals have no detectable Nrf2 levels in their skin, whereas skin isolated from Keap1-KD SKH-1 hairless mice has ~2-fold higher levels of the transcription factor compared to WT (Fig. 1C). The specific activity of the Nrf2-dependent enzyme NAD(P)H:quinone oxidoreductase 1 (NQO1) is ~30% lower ($p < 0.05$) in Nrf2-KO compared to WT skin, whereas it is 2.2-fold higher in Keap1-KD skin ($p < 0.001$) (Fig. 1D). Similarly, compared to WT, the specific activity of cutaneous glutathione *S*-transferase (GST), another Nrf2-target enzyme, is reduced

11

by ~40% in Nrf2-KO mice ($p < 0.05$), and upregulated by 1.3-fold in Keap1-knockdown animals ($p < 0.05$) (Fig. 1D). The protein levels of the catalytic subunit of γ-glutamyl cysteine ligase (GCLC), an Nrf2-dependent enzyme which catalyzes the rate-limiting step in glutathione biosynthesis, are not vastly different between Nrf2-KO and WT skin; however they are ~3.6-fold higher in the skin of Keap1-KD mice (Fig. 1E). The mRNA levels for heme oxygenase 1 (HMOX1) do not differ significantly between skin samples of Nrf2-KO and WT mice, but are 1.6-fold higher ($p < 0.05$) in the skin of Keap1-KD mice (Fig. 1F).

The relatively modest effect of the absence of functional Nrf2 on target gene expression is surprising. It suggests that skin cells may have adapted alternate antioxidant response mechanisms which help them to maintain homeostasis in the face of environmental stresses. Two possible candidates to compensate for the lack of Nrf2 function are Nrf1 and Nrf3, members of the same family of cap'n'collar basic-region leucine zipper transcription factors. Quantitative real-time PCR analysis showed that whilst the mRNA levels for Nrf1 were not significantly different among the genotypes (Fig. S2A), the mRNA levels for Nrf3 were indeed upregulated (by 1.5-fold, $p < 0.001$) compared to WT in skin samples of Nrf2-KO mice (Fig. S2B). This finding is in full agreement with the previously reported upregulation of Nrf3 in the skin of Nrf2-knockout mice of a different (mixed) genetic background (30).

Next, we tested the ability of TBE-31 (Fig. 2A), one of the most potent Nrf2 activators known to date (21, 31), to stabilize Nrf2 and induce target gene expression in the skin of mice of the three genotypes. Five daily topical applications of TBE-31 (200 nmol per mouse, 24 h apart) led to a robust stabilization of Nrf2 in the skin of WT mice (Fig. 1C). This response was diminished in Keap1-KD animals, and completely absent in Nrf2-deficient mice, confirming that the Keap1/Nrf2 pathway is the primary target for this compound. In the skin of WT mice, the mRNA levels for the Nrf2-target enzymes NQO1, GCLC and GSTP

12

were upregulated by 8-, 1.8-, and 1.9-fold, respectively ($p < 0.001$) (Fig. 2B). In close

agreement, the cutaneous NQO1 and GST specific enzyme activities were elevated by 6- ($p < 0.01$) and 1.8-fold ($p < 0.01$), respectively 24 h after the last treatment with TBE-31 (Fig. 2C).

In contrast to WT, no induction of NQO1 by TBE-31 was seen in skin of Nrf2-KO mice (Fig. S3A). Importantly, induction was not limited to the epidermis (6.9-fold, $p < 0.001$), as it was

clearly observed in the dermis, albeit to a smaller (2.5-fold, $p < 0.001$) degree (Fig. S3B).

Having established the effect of the Nrf2 status on both basal and inducible

expression of its classical target genes in the mouse skin, we then exposed WT mice to a

single acute dose of solar-simulated UV radiation and observed dose-dependent changes in

the appearance of the skin vasculature 24 h after exposure (Fig. 3A). We used UV radiation

sources with properties nearly identical to the UV component of the sunlight that reaches the

surface of the Earth, comprising 5% UVB and 95% UVA wavelengths (Fig. S1). The gene

expression of the pro-inflammatory cytokine interleukin (IL)-6 was dramatically and dose-

dependently induced by 16-, 129-, and 170-fold ($p < 0.001$) 24 h after solar-simulated UV

radiation delivering 200-, 400-, and 600 mJ/cm^2 of UVB, respectively (Fig. 3B). The onset of

skin inflammation was further confirmed by the dose-dependent upregulation of IL-1β, the

levels of which increased by 3-, 16-, and 15-fold ($p < 0.05$) (Fig. 3C). Comparison of the UV

radiation-provoked inflammatory responses among mice from the three genotypes revealed

that disruption of Nrf2 did not lead to appreciable differences in comparison with WT, but its

constitutive upregulation significantly suppressed the production of both pro-inflammatory

cytokines. Thus, compared to WT, 24 h after irradiation, the upregulation of IL-6 and IL-1β

was reduced by 74- ($p < 0.01$) and 48% ($p < 0.05$), respectively in the skin of Keap1-KD

mice (Fig. 3D,E). Analysis of cellular infiltrates from the affected skin areas showed no

significant difference in the total amount of recruited CD45+ cells between WT and Keap1-

KD animals (Fig. S4). Of note, there was a slight indication of attenuated CD11b+Gr1+ cells

13

recruitment in the skin of Keap1-KD mice, suggesting reduced neutrophil presence, however this did not reach statistical significance. Remarkably, 72 h after exposure to solar-simulated UV radiation, when erythema development was most obvious, the skin of the Keap1-KD animals showed no apparent erythema, in sharp contrast with the skin of their WT and Nrf2-KO counterparts (Fig. 3F). There were no apparent differences in the skin of mutant mice, including epidermal thickness, and the skin architecture of animals of all genotypes appeared very similar and histologically normal (Fig. S5). Together, these results demonstrate the protective role of genetic upregulation of Nrf2 against inflammation caused by solar-simulated UV radiation.

Genetic upregulation of Nrf2 protects against skin carcinogenesis caused by solar-simulated UV radiation

The critical role of inflammation for all stages of tumor development is well established (32). In particular, IL-6 is one of the best-characterized pro-tumorigenic cytokines, and has been recently proposed to be a new target for cancer therapy (33). As Keap1-KD mice showed a very substantial reduction in induction of IL-6 expression provoked by solar-simulated UV radiation (Fig. 3D) and they also express higher levels of cytoprotective enzymes in their skin (Fig. 1D-F) than their WT or Nrf2-KO counterparts, we hypothesized that Keap1-KD mice will be protected against skin carcinogenesis in comparison with WT or Nrf2-KO animals. Conversely, because Nrf2-KO were not substantially different from WT mice in terms of inflammatory responses to solar-simulated UV radiation (Fig. 3D-F), they were expected not to be significantly different from WT with respect to development of skin tumors. To test this hypothesis, we subjected groups of 30 mice of each of the three genotypes to chronic exposure to sub-erythemal doses of solar-simulated UV radiation (comprised of 2 J/cm^2 UVA and 90 mJ/cm^2 UVB), twice a week for 15 weeks. Tumor

14

development was then followed during the subsequent 20 weeks. Notably, the

histopathological spectrum of the tumors which form in this mouse model closely resembles

the spectrum of human cSCC, including well-, moderately-, and poorly-differentiated tumors

(Fig. 4A).

In agreement with the lack of profound differences in expression of Nrf2 downstream

target genes (Fig. 1D-F) and solar-simulated UV radiation-mediated induction in pro-

inflammatory cytokines (Fig. 3D,E) between Nrf2-KO and WT mice, there were no

significant differences in tumor incidence, multiplicity, or burden between these two

genotypes (Fig. 4B-D). In sharp contrast, the Keap1-KD mice were substantially protected

against the carcinogenic effects of solar-simulated UV radiation. Thus, whereas 50% of WT

and Nrf2-KO mice had tumors at treatment week 24 (i.e. 9 weeks after the UV radiation

schedule was discontinued), it took nearly twice as long (i.e. 16 weeks, or treatment week 30)

for 50% of the Keap1-KD mice to develop their first tumor (Fig. 4B). At the end of the

experiment, more than 90% of the WT and Nrf2-KO animals had tumors, whereas tumor

incidence was 60% in the Keap1-KD mice. Kaplan–Meier 'survival analysis' applied to

freedom-from-tumors, followed by a log-rank test for equality of survivor function showed a

highly significant difference between the Keap1-KD and the WT groups ($\chi2 = 25.9$; p <

0.0001). The effect of genetic Nrf2 upregulation on tumor multiplicity was even more

profound, and there was a ~5-fold reduction, from 5.4 tumors per mouse in the WT group to

1 tumor per mouse in the Keap1-KD group (Fig. 4C). The difference between groups was

highly significant by ANOVA followed by Bartlett's test for equal variances (F 80.18, p

<0.0001), and even stronger for comparison of just the Keap1-KD group with the WT group

(F 157.59, p<0.0001). The Keap1-KD group became significantly different from the WT

group by week 23. The total tumor volume (expressed in mm^3) per mouse was also

profoundly affected by the genetic upregulation of Nrf2 (Fig. 4D), and there was a significant

15

80% reduction between the Keap1-KD and the WT groups over the last 3 weeks of the experiment (i.e. treatment weeks 33-35) (F 9.36, p<0.0022).

Pharmacological activation of Nrf2 protects against inflammation caused by solar-simulated UV radiation

To test whether similar to genetic, pharmacological Nrf2 activation can also protect against solar-simulated UV radiation-mediated inflammation, we used TBE-31. At low nanomolar concentrations, this acetylenic tricyclic bis(cyano enone) compound induces cytoprotective enzymes and inhibits IFNγ-mediated pro-inflammatory responses (21, 31, 34). Three daily topical applications of 40 nmol of TBE-31, every 24 hours, did not affect the expression of IL-6, IL-1β, or prostaglandin-endoperoxide synthase (more commonly known as cyclooxygenase 2, or COX-2) in non-irradiated murine skin (Fig. 5A-C). However, after exposure to solar-simulated UV radiation, the mRNA levels for the there inflammatory markers were lower in the skin of TBE-31- than in vehicle-treated mice (Fig. 5D-F). Thus, compared to vehicle treatment, 24 h after irradiation, the upregulation of IL-6, IL-1β, and COX2 was decreased by 55- ($p < 0.001$), 24- ($p < 0.05$), and 30% ($p < 0.05$), respectively in the skin of TBE-31-treated mice. The protective effect of TBE-31 against UV radiation-induced inflammation was largely absent in Nrf2-KO mice (Fig. 5G-I), although there was an apparent non-statistically significant protection against IL-1β upregulation in the skin of Nrf2-KO mice (Fig. 5H), in agreement with our previous report that some, but not all of the anti-inflammatory effects of compounds of this type are Nrf2-dependent (35).

Pharmacological activation of Nrf2 protects against skin carcinogenesis caused by solar-simulated UV radiation during azathioprine treatment

16

Azathioprine is a highly effective anti-inflammatory and immunosuppressive agent that is widely used for the treatment of inflammatory bowel disease and in solid organ transplantation. Its active metabolite, 6-thioguanine (6-TG) incorporates in genomic DNA during replication. The combination of 6-TG and UVA radiation is highly mutagenic, and increases the sensitivity of the human skin to UVA radiation (36). 6-TG is a UVA photosensitizer, leading to formation of reactive oxygen species (ROS) which cause oxidative damage to DNA and proteins, including DNA damage repair enzymes, thus compromizing DNA break rejoining and base and nucleotide excision repair (37). These findings have provided a direct causative link between thiopurine therapies and the associated increased (by more than 100-fold relative to the general population) risk for highly aggressive cSCC.

To test whether activation of Nrf2 can protect against solar-simulated UV radiation-mediated skin carcinogenesis under conditions of azathioprine therapy, we used a pharmacological approach. We have previously shown that TBE-31, at low nanomolar concentrations, protects cultured murine keratinocytes (Kera-308 cells) against generation of ROS after exposure to 6-TG (a surrogate for azathioprine) and UVA radiation (38). Importantly, the protective effect of TBE-31 correlated with a robust upregulation of the activities of the Nrf2-target enzymes NQO1 and GST. Because ROS are important mediators of the mutagenic effects of the combination of 6-TG and UV radiation (39), and TBE-31 effectively reduced inflammation in mice exposed to solar-simulated UV radiation (Fig. 5), together these data suggest that TBE-31 is a good candidate for a pharmacological protective agent against UV radiation-mediated skin carcinogenesis under conditions of azathioprine therapy.

Based on detailed pharmacokinetics and dose optimization experiments (Supplemental Results and Fig. S6 and S7), we began administering TBE-31 (40 nmol/mouse/day, topically, 2 days/week) simultaneously with azathioprine (1 mg/kg/day in

17

the drinking water) two weeks before the start of the irradiation schedule, and continued applying both TBE-31 and azathioprine at this dosing regimen throughout the duration of the experiment (a total of 33 weeks). Similar to the experiment with the three genotypes of mice, the animals were exposed to chronic sub-erythemal solar-simulated UV radiation (comprised of 2 J/cm^2 UVA and 90 mJ/cm^2 UVB). Notably, these solar-simulated UV radiation sources have a peak emission at 340 nm (Fig. S1), which coincides with the absorption peak of 6-TG, the active metabolite of azathioprine (39). After bi-weekly exposures for 15 weeks, irradiation was discontinued, and tumor development was evaluated during the subsequent 16 weeks.

Whereas tumor incidence was not significantly different between the control and the TBE-31-treated groups (Fig. 6A), TBE-31 significantly reduced tumor multiplicity (Fig. 6B). Kaplan–Meier survival analysis applied to freedom-from-tumors, followed by a log-rank test for equality of survivor function showed no significant difference between groups. However, the differences in average tumor number were highly significant (F 39.11, p<0.0001) by oneway ANOVA followed by Bartlett's test for equal variances, with the control group ultimately having 9.5 tumors per mouse, compared to 5.3 tumors per mouse for the TBE-treated group; differences in tumor number became significant at week 23. Moreover, the protective effect of TBE-31 was especially striking with respect to tumor volume, which was markedly reduced (~5-fold), from 225 mm^3 per mouse in the vehicle-treated group to 41.9 mm^3 in the TBE-31- treated group (Fig. 6C). The difference between the groups was highly significant (F 18.16, p<0.0001) by oneway ANOVA followed by Bartlett's test for equal variances.

18

Topical application of extracts containing the Nrf2 activator sulforaphane protects healthy human subjects against skin erythema development caused by solar-simulated UV radiation

In a proof-of-principle study with six healthy human subjects, we have previously shown that, compared to vehicle-treated sites, the intensity of narrow-band (311 nm) UVB radiation-induced skin erythema was reduced by around 40% at sites that received topical treatment with broccoli extracts delivering the naturally-occurring Nrf2 activator sulforaphane (15). As TBE-31 is a synthetic compound which has not yet been approved for use in humans, we used sulforaphane-rich broccoli extracts to test the hypothesis that, as in mice, pharmacological activation of Nrf2 will protect humans against skin damage by solar-simulated UV radiation. Skin erythema was employed as a quantifiable surrogate end-point for cutaneous damage and skin cancer risk (40).

The study was randomized, double blind, and placebo-controlled (Fig. 7A). We compared the response of the skin of 24 healthy human volunteers, men and women, to different wavebands of monochromator UV radiation and solar-simulated UV waveband radiation after topical application of extracts containing either sulforaphane (SF, active) or the inactive precursor of sulforaphane, glucoraphanin (GR, placebo) (Fig. S8 and S9), in a double-blind side-by-side comparison, with each subject acting as his/her own control. We applied in a randomized fashion to the right or the left half of the mid-upper back skin (avoiding the paravertebral area) of each volunteer either active or placebo extract containing 200 nmol/cm^2 of sulforaphane or glucoraphanin, respectively, 3 times, 24 h apart. The choice of this dose was based on our previous studies in which we showed that sulforaphane caused a dose-dependent induction of NQO1 in human skin punch biopsies (41). The study was conducted on an outpatient basis, because prior experience had indicated no significant adverse reactions of the human skin to application of these doses of the extracts. Twenty-four

19

hours after the last extract applications, small areas of the skin (approximately 1 cm^2) within

the extract-treated areas were exposed to a range of doses of monochromatic UV radiation

and visible light, and solar-simulated UV radiation according to a standardized solar

simulator phototesting technique that is used routinely in the Photobiology Unit at Ninewells

Hospital, Dundee, Scotland, United Kingdom (42). Skin responses to each dose of radiation

were assessed 24 h after irradiation by using a semi-quantitative visual scale and quantifying

objectively the resulting erythema using an erythema meter. Critically, those making the

erythema measurements were blinded to treatment, allowing for an unbiased objective

comparison of the degrees of erythemal response between active- and placebo-treated areas.

Because we used a series of radiation doses for each subject, we calculated the sum of

erythema, rather than simply taking the intensity of erythema at 24 h after a particular dose.

This process takes into account individual differences in erythemal sensitivity in terms of

both the threshold and slope of response. No significant differences in threshold responses,

i.e. minimal erythemal dose (MED), were observed at any of the wavelengths. However,

mean erythema sum after testing with one of the wavebands (the solar-simulator) for the

placebo-treated sites was 91, compared with 59 for the active-treated sites, a difference in

mean erythema of 31 (95% confidence interval 6 to 58; p = 0.02) (Fig. 7B). Thus, compared

to placebo-treated areas of the skin, the overall erythemal response was reduced by 35% at

areas that had received the pharmacological Nrf2 activator.

Discussion

Exome sequencing of human primary cSCC and matched normal tissue has revealed

an extraordinary large mutation burden of approximately 1,300 somatic single-nucleotide

variants per exome (13), making the possibility for success of a single-target therapy unlikely,

and highlighting the need for agents capable of affecting multiple hallmarks of cancer. Nrf2-

20

dependent cytoprotective responses provide broad, versatile, and long-lasting protection that counteracts many of the damaging effects of solar UV radiation, a complete carcinogen which can cause the initiation, promotion and progression of cSCC. Because of its crucial role in cytoprotection, including regulation of the cellular redox homeostasis, Nrf2 is now considered a drug target (43). However, the frequent activation of Nrf2 in established human tumors has raised the critical question whether Nrf2 may also be a driver in cancer.

Using the oncogenic H-Ras(Q61L)-driven DMBA/TPA model, it has been shown that skin carcinogenesis is enhanced in mice which are either deficient for Nrf2 (16) or express a dominant negative form of Nrf2 in the epidermis (44). This mutant H-Ras-driven chemical carcinogenesis model gives rise primarily to benign papillomas, and is very different from the solar UV radiation-induced cutaneous squamous cell carcinoma, in which H-Ras mutations are rare (45). By generating SKH-1 hairless mice in which Nrf2 is either disrupted (Nrf2-KO SKH-1 hairless) or constitutively upregulated (Keap1-KD SKH-1 hairless), and using chronic twice-weekly exposures to solar-simulated UV radiation as the carcinogen, we addressed the role of Nrf2 in solar UV radiation-induced skin carcinogenesis. To our knowledge, Keap1-KD mice on any genetic background have not been previously used in any carcinogenesis model. Importantly, the extent of activation of Nrf2 in both models (genetic and pharmacological) described in this contribution does not cause any obvious skin abnormalities (Fig. S5) and furthermore, is comparable to the level of pharmacological Nrf2 activation which is achievable in the human skin (41). This is in contrast to the very high levels of Nrf2 activity that are seen in the skin of mice genetically engineered to express keratinocyte-specific constitutively active mutant Nrf2 under the control of a β-actin promoter and a CMV enhancer, the expression of which causes sebaceous gland hypertrophy, hyperkeratosis and cyst formation (46). We found that genetic or pharmacological activation of Nrf2 results in higher expression of cytoprotective enzymes, suppression of UV radiation-

21

evoked pro-inflammatory responses, and marked reduction in tumor growth. Importantly, the

protective effect of Nrf2 activation is evident in both immunocompetent mice as well as in

animals that are receiving life-long treatment with the immunosuppressive agent azathioprine.

This finding indicates that pharmacological activation of Nrf2 could be an effective strategy

for protection against cSCC in both the general population and in high-risk groups, such as

organ transplant recipients and inflammatory bowel disease patients, and encourage the

clinical development of potent and specific Nrf2 activators, such as TBE-31. This conclusion

is further strengthened by the fact that, in healthy human subjects, pharmacological activation

of Nrf2 is protective against solar-simulated UV radiation-evoked erythema, a surrogate

marker for cutaneous photodamage and skin cancer risk (40).

It was recently demonstrated that Nrf2 directs carbon flux toward the pentose

phosphate pathway and the tricarboxylic acid cycle, and furthermore, during sustained

activation of PI3K-Akt signaling, this transcription factor redirects glucose and glutamine

into anabolic pathways (47, 48). In addition, it has been shown that following expression of

endogenous oncogenic alleles of K-Ras, B-Raf and Myc, transcription of Nrf2 is increased,

whereas the number of neoplastic cells in the pancreas produced by transgenic expression of

oncogenic K-Ras(G12D) and their proliferation rate are decreased in Nrf2-KO mice in

comparison with their WT counterparts (49). Curiously, dietary supplementation with the

antioxidants *N*-acetylcysteine or vitamin E accelerates tumor progression and decreases

survival in mouse models of oncogenic B-Raf- and K-Ras-induced lung cancer, and RNA

sequencing has revealed changes in tumor transcriptome profiles that are characterized by

reduced expression of Nrf2-dependent antioxidant genes (50). Together with these findings,

the results from the present study imply that Nrf2 is not a driver for skin carcinogenesis and

strongly suggest that this is very likely also to be the case for other malignancies. Rather, the

frequent activation of Nrf2 that is seen in many established human tumors is a marker of

22

metabolic adaptation that allows growth and survival under conditions of disrupted metabolic balance and compromised redox and energy homeostasis.

23

References

1. Kensler TW, Wakabayashi N, Biswal S. Cell survival responses to environmental stresses via the Keap1-Nrf2-ARE pathway. Annu Rev Pharmacol Toxicol. 2007;47:89-116.

2. Taguchi K, Motohashi H, Yamamoto M. Molecular mechanisms of the Keap1-Nrf2 pathway in stress response and cancer evolution. Genes Cells. 2011;16:123-40.

3. Talalay P, Dinkova-Kostova AT, Holtzclaw WD. Importance of phase 2 gene regulation in protection against electrophile and reactive oxygen toxicity and carcinogenesis. Adv Enzyme Regul. 2003;43:121-34.

4. Hayes JD, Dinkova-Kostova AT. The Nrf2 regulatory network provides an interface between redox and intermediary metabolism. Trends Biochem Sci. 2014;39:199-218.

5. Cullinan SB, Gordan JD, Jin J, Harper JW, Diehl JA. The Keap1-BTB protein is an adaptor that bridges Nrf2 to a Cul3-based E3 ligase: oxidative stress sensing by a Cul3-Keap1 ligase. Mol Cell Biol. 2004;24:8477-86.

6. Zhang DD, Lo SC, Cross JV, Templeton DJ, Hannink M. Keap1 is a redox-regulated substrate adaptor protein for a Cul3-dependent ubiquitin ligase complex. Mol Cell Biol. 2004;24:10941-53.

7. Kobayashi A, Kang MI, Okawa H, Ohtsuji M, Zenke Y, Chiba T, et al. Oxidative stress sensor Keap1 functions as an adaptor for Cul3-based E3 ligase to regulate proteasomal degradation of Nrf2. Mol Cell Biol. 2004;24:7130-9.

8. Dinkova-Kostova AT, Holtzclaw WD, Cole RN, Itoh K, Wakabayashi N, Katoh Y, et al. Direct evidence that sulfhydryl groups of Keap1 are the sensors regulating induction of phase 2 enzymes that protect against carcinogens and oxidants. Proc Natl Acad Sci U S A. 2002;99:11908-13.

9. McMahon M, Lamont DJ, Beattie KA, Hayes JD. Keap1 perceives stress via three sensors for the endogenous signaling molecules nitric oxide, zinc, and alkenals. Proc Natl Acad Sci U S A. 2010;107:18838-43.

10. Suzuki T, Motohashi H, Yamamoto M. Toward clinical application of the Keap1-Nrf2 pathway. Trends Pharmacol Sci. 2013;34:340-6.

11. Jaramillo MC, Zhang DD. The emerging role of the Nrf2-Keap1 signaling pathway in cancer. Genes Dev. 2013;27:2179-91.

12. Narayanan DL, Saladi RN, Fox JL. Ultraviolet radiation and skin cancer. International journal of dermatology. 2010;49:978-86.

13. Durinck S, Ho C, Wang NJ, Liao W, Jakkula LR, Collisson EA, et al. Temporal dissection of tumorigenesis in primary cancers. Cancer discovery. 2011;1:137-43.

14. Harwood CA, Mesher D, McGregor JM, Mitchell L, Leedham-Green M, Raftery M, et al. A surveillance model for skin cancer in organ transplant recipients: a 22-year prospective study in an ethnically diverse population. Am J Transplant. 2013;13:119-29.

15. Talalay P, Fahey JW, Healy ZR, Wehage SL, Benedict AL, Min C, et al. Sulforaphane mobilizes cellular defenses that protect skin against damage by UV radiation. Proc Natl Acad Sci U S A. 2007;104:17500-5.

16. Xu C, Huang MT, Shen G, Yuan X, Lin W, Khor TO, et al. Inhibition of 7,12-dimethylbenz(a)anthracene-induced skin tumorigenesis in C57BL/6 mice by sulforaphane is mediated by nuclear factor E2-related factor 2. Cancer Res. 2006;66:8293-6.

17. Gills JJ, Jeffery EH, Matusheski NV, Moon RC, Lantvit DD, Pezzuto JM. Sulforaphane prevents mouse skin tumorigenesis during the stage of promotion. Cancer Lett. 2006;236:72-9.

18. Dinkova-Kostova AT, Jenkins SN, Fahey JW, Ye L, Wehage SL, Liby KT, et al. Protection against UV-light-induced skin carcinogenesis in SKH-1 high-risk mice by sulforaphane-containing broccoli sprout extracts. Cancer Lett. 2006;240:243-52.

19. Dinkova-Kostova AT, Fahey JW, Benedict AL, Jenkins SN, Ye L, Wehage SL, et al. Dietary glucoraphanin-rich broccoli sprout extracts protect against UV radiation-induced skin carcinogenesis in SKH-1 hairless mice. Photochem Photobiol Sci. 2010;9:597-600.

20. Benavides F, Oberyszyn TM, VanBuskirk AM, Reeve VE, Kusewitt DF. The hairless mouse in skin research. J Dermatol Sci. 2009;53:10-8.

21. Honda T, Yoshizawa H, Sundararajan C, David E, Lajoie MJ, Favaloro FG, Jr., et al. Tricyclic compounds containing nonenolizable cyano enones. A novel class of highly potent anti-inflammatory and cytoprotective agents. J Med Chem. 2011;54:1762-78.

22. Saito A, Zheng S, Takahashi M, Li W, Ojima I, Honda T. An improved synthesis of a hydroxymethyl tricyclicketone from cyclohexanone, the key process for the synthesis of a highly potent anti-inflammatory and cytoprotective agent. Synthesis 2013;45:3251-4.

23. Zheng S, Huang JT, Knatko EV, Sharp S, Higgins M, Ojima I, et al. Synthesis of (13) C2 (15) N2 -labeled anti-inflammatory and cytoprotective tricyclic bis(cyanoenone) ([(13) C2 (15) N2]-TBE-31) as an internal standard for quantification by stable isotope dilution LC-MS method. Journal of labelled compounds & radiopharmaceuticals. 2014;57:606-10.

24. Itoh K, Chiba T, Takahashi S, Ishii T, Igarashi K, Katoh Y, et al. An Nrf2/small Maf heterodimer mediates the induction of phase II detoxifying enzyme genes through antioxidant response elements. Biochem Biophys Res Commun. 1997;236:313-22.

25. Taguchi K, Maher JM, Suzuki T, Kawatani Y, Motohashi H, Yamamoto M. Genetic analysis of cytoprotective functions supported by graded expression of Keap1. Mol Cell Biol. 2010;30:3016-26.

26. Prochaska HJ, Santamaria AB. Direct measurement of NAD(P)H:quinone reductase from cells cultured in microtiter wells: a screening assay for anticarcinogenic enzyme inducers. Anal Biochem. 1988;169:328-36.

27. Habig WH, Jakoby WB. Glutathione S-transferases (rat and human). Methods Enzymol. 1981;77:218-31.

28. McMahon M, Itoh K, Yamamoto M, Hayes JD. Keap1-dependent proteasomal degradation of transcription factor Nrf2 contributes to the negative regulation of antioxidant response element-driven gene expression. J Biol Chem. 2003;278:21592-600.

29. Wade KL, Garrard IJ, Fahey JW. Improved hydrophilic interaction chromatography method for the identification and quantification of glucosinolates. J Chromatogr A. 2007;1154:469-72.

30. Braun S, Hanselmann C, Gassmann MG, auf dem Keller U, Born-Berclaz C, Chan K, et al. Nrf2 transcription factor, a novel target of keratinocyte growth factor action which regulates gene expression and inflammation in the healing skin wound. Mol Cell Biol. 2002;22:5492-505.

31. Dinkova-Kostova AT, Talalay P, Sharkey J, Zhang Y, Holtzclaw WD, Wang XJ, et al. An exceptionally potent inducer of cytoprotective enzymes: elucidation of the structural features that determine inducer potency and reactivity with Keap1. J Biol Chem. 2010;285:33747-55.

32. Grivennikov SI, Greten FR, Karin M. Immunity, inflammation, and cancer. Cell. 2010;140:883-99.

33. Taniguchi K, Karin M. IL-6 and related cytokines as the critical lynchpins between inflammation and cancer. Semin Immunol. 2014;26:54-74.

34. Liby K, Yore MM, Roebuck BD, Baumgartner KJ, Honda T, Sundararajan C, et al. A novel acetylenic tricyclic bis-(cyano enone) potently induces phase 2 cytoprotective pathways and blocks liver carcinogenesis induced by aflatoxin. Cancer Res. 2008;68:6727-33.

35. Liu H, Dinkova-Kostova AT, Talalay P. Coordinate regulation of enzyme markers for inflammation and for protection against oxidants and electrophiles. Proc Natl Acad Sci U S A. 2008;105:15926-31.

36. O'Donovan P, Perrett CM, Zhang X, Montaner B, Xu YZ, Harwood CA, et al. Azathioprine and UVA light generate mutagenic oxidative DNA damage. Science. 2005;309:1871-4.

37. Gueranger Q, Li F, Peacock M, Larnicol-Fery A, Brem R, Macpherson P, et al. Protein Oxidation and DNA Repair Inhibition by 6-Thioguanine and UVA Radiation. J Invest Dermatol. 2014;134:1408-17.

38. Kalra S, Knatko EV, Zhang Y, Honda T, Yamamoto M, Dinkova-Kostova AT. Highly potent activation of Nrf2 by topical tricyclic bis(cyano enone): implications for protection against UV radiation during thiopurine therapy. Cancer Prev Res (Phila). 2012;5:973-81.

39. Karran P, Attard N. Thiopurines in current medical practice: molecular mechanisms and contributions to therapy-related cancer. Nat Rev Cancer. 2008;8:24-36.

40. de Gruijl FR, Van der Leun JC. Estimate of the wavelength dependency of ultraviolet carcinogenesis in humans and its relevance to the risk assessment of a stratospheric ozone depletion. Health Phys. 1994;67:319-25.

41. Dinkova-Kostova AT, Fahey JW, Wade KL, Jenkins SN, Shapiro TA, Fuchs EJ, et al. Induction of the phase 2 response in mouse and human skin by sulforaphane-containing broccoli sprout extracts. Cancer Epidemiol Biomarkers Prev. 2007;16:847-51.

42. Dawe RS, Ibbotson SH, Sanderson JB, Thomson EM, Ferguson J. A randomized controlled trial (volunteer study) of sitafloxacin, enoxacin, levofloxacin and sparfloxacin phototoxicity. The British journal of dermatology. 2003;149:1232-41.

43. Crunkhorn S. Deal watch: Abbott boosts investment in NRF2 activators for reducing oxidative stress. Nature reviews Drug discovery. 2012;11:96.

44. auf dem Keller U, Huber M, Beyer TA, Kumin A, Siemes C, Braun S, et al. Nrf transcription factors in keratinocytes are essential for skin tumor prevention but not for wound healing. Mol Cell Biol. 2006;26:3773-84.

45. South AP, Purdie KJ, Watt SA, Haldenby S, den Breems NY, Dimon M, Arron ST, Kluk MJ, Aster JC, McHugh A, Xue DJ, Dayal JH, Robinson KS, Rizvi SM, Proby CM, Harwood CA, Leigh IM. NOTCH1 mutations occur early during cutaneous squamous cell carcinogenesis. J Invest Dermatol. 2014;134:2630-8.

46. Schafer M, Willrodt AH, Kurinna S, Link AS, Farwanah H, Geusau A, et al. Activation of Nrf2 in keratinocytes causes chloracne (MADISH)-like skin disease in mice. EMBO Mol Med. 2014;6:442-57.

47. Mitsuishi Y, Taguchi K, Kawatani Y, Shibata T, Nukiwa T, Aburatani H, et al. Nrf2 redirects glucose and glutamine into anabolic pathways in metabolic reprogramming. Cancer Cell. 2012;22:66-79.

48. Singh A, Happel C, Manna SK, Acquaah-Mensah G, Carrerero J, Kumar S, et al. Transcription factor NRF2 regulates miR-1 and miR-206 to drive tumorigenesis. J Clin Invest. 2013;123:2921-34.

26

49. DeNicola GM, Karreth FA, Humpton TJ, Gopinathan A, Wei C, Frese K, et al.
    Oncogene-induced Nrf2 transcription promotes ROS detoxification and tumorigenesis.
    Nature. 2011;475:106-9.
50. Sayin VI, Ibrahim MX, Larsson E, Nilsson JA, Lindahl P, Bergo MO. Antioxidants
    accelerate lung cancer progression in mice. Sci Transl Med. 2014;6:221ra15.

Figure Legends

Figure 1. Genetic upregulation of Nrf2 in the skin of SKH-1 hairless mice leads to enhanced expression of Nrf2-target genes. Quantitative real-time PCR analysis of mRNA (**A**) and representative immunoblots (n=3) (**B**) of Keap1 from skin samples of WT, Nrf2-KO and Keap1-KD SKH-1 hairless mice (n=3). (**C**) Representative immunoblots (n=3) of Nrf2 levels in skin of vehicle (80% acetone)- or TBE-31 (five daily doses of 200 nmol per mouse, every 24 h)-treated WT, Keap1-KD and Nrf2-KO SKH-1 hairless mice. (**D-F**) Cutaneous NQO1 (menadione as a substrate) and GST (CDNB as a substrate) specific activity (**D**), GCLC protein levels (**E**), and HMOX1 mRNA levels (**F**) in WT, Nrf2-KO and Keap1-KD SKH-1 hairless mice (n=3). Data were normalized with respect to WT levels. Results are means ± S.D. *, $p < 0.001$ for comparisons between WT and mutant skin. The numbers shown in the western blots represent the ratio of the intensity of each band to that of the corresponding loading control, normalized to one of the wild-type samples.

Figure 2. Pharmacological upregulation of Nrf2 in the skin of SKH-1 hairless mice leads to enhanced expression of Nrf2-target genes. (**A**) Chemical structure of TBE-31. (**B,C**) Quantitative real-time PCR analysis of mRNA of NQO1, GSTP, and GCLC (**B**) and NQO1 (menadione as a substrate) and GST (CDNB as a substrate) specific activity (**C**) in skin samples of vehicle (80% acetone)- or TBE-31 (five daily doses of 200 nmol per mouse, every 24 h, applied topically over the entire back of the animals)-treated WT SKH-1 hairless mice, n=3). Data were normalized with respect to vehicle-treated levels. Results are means ± S.D. *, $p < 0.001$ for comparisons between vehicle- and TBE-treated skin.

Figure 3. Genetic upregulation of Nrf2 in the skin of SKH-1 hairless mice protects against inflammation caused by solar-simulated UV radiation. (**A**) Images of the dorsal
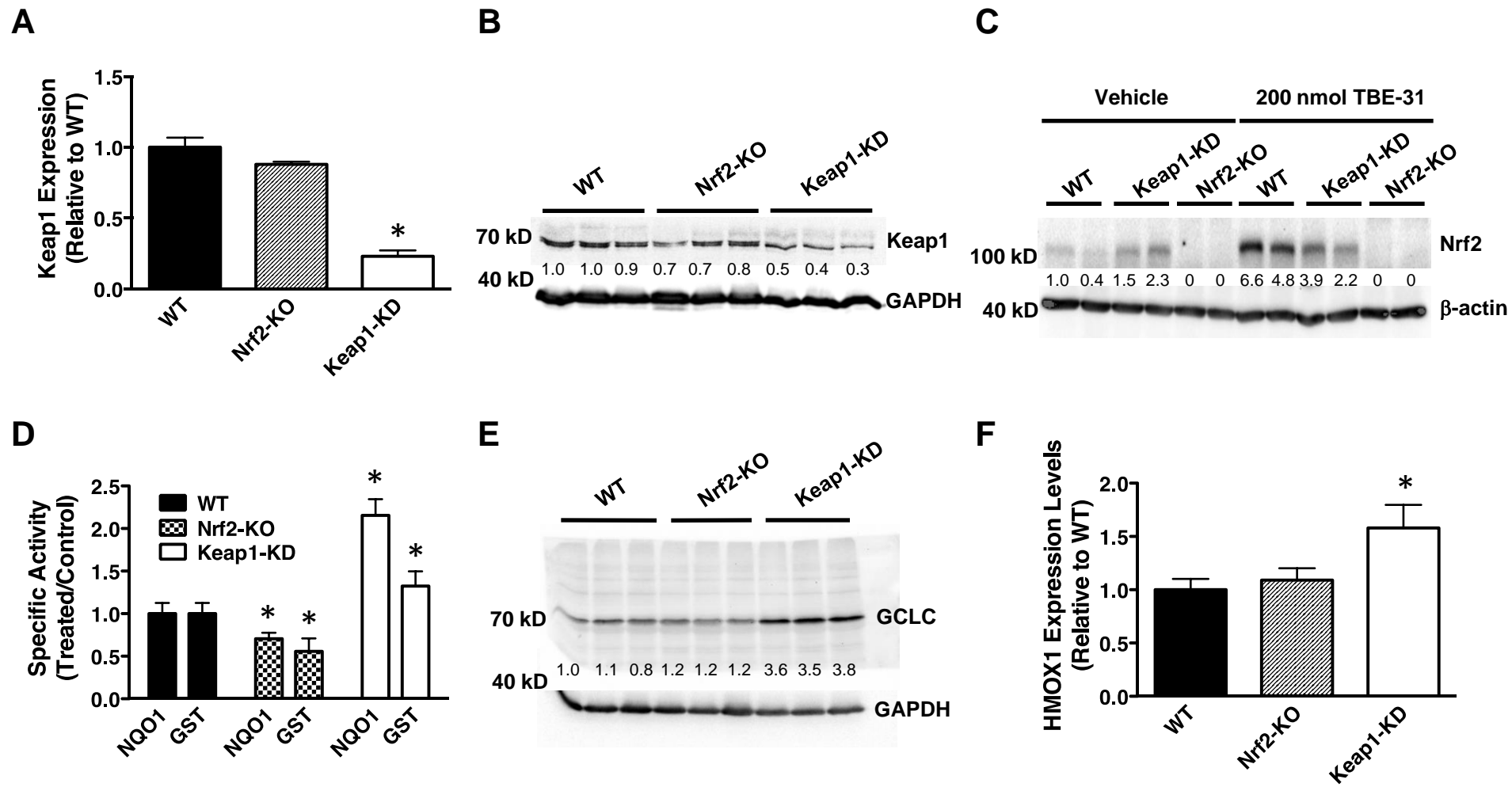
28

skin vasculature of 12 individual animals (4 groups of 3, arranged in columns) used for

analyses of the inflammatory markers shown in (**B**) and (**C**). Quantitative real-time PCR

analysis of cutaneous mRNA levels of IL-6 (**B**) and IL-1β (**C**) of WT SKH-1 hairless mice

(n=3) 24 h after acute exposure to a single dose (the indicated doses refer to the UVB

component) of solar-simulated UV radiation. Quantitative real-time PCR analysis of mRNA

of IL-6 (**D**) and IL-1β (**E**) in skin samples of WT, Nrf2-KO and Keap1-KD SKH-1 hairless

mice (n=3) 24 h after acute exposure to a single dose (UVB component = 400 mJ/cm^2) of

solar-simulated UV radiation. Data were normalized with respect to levels in non-irradiated

skin. Results are means ± S.D. *, $p < 0.05$. (**F**) Photographs of WT, Nrf2-KO and Keap1-KD

SKH-1 hairless mice showing delayed erythemal response 72 h after irradiation.

**Figure 4. Genetic upregulation of Nrf2 protects against cutaneous carcinogenesis
mediated by solar-simulated UV radiation.** (**A**) Histopathology of tumors which form after

chronic exposure to solar-simulated UV radiation in SKH-1 hairless mice. Examples are

shown of epithelial lesions, including pre-malignant epidermal hyperplasia, well-

differentiated non-invasive, and moderately-differentiated early-invasive cSCC. Scale bar =

200 μm. (**B-D**) WT, Nrf2-KO and Keap1-KD SKH-1 hairless mice (n=30, with every cage

housing representatives of each genotype) were exposed chronically to solar-simulated UV

radiation (comprised of 2 J/cm^2 UVA and 90 mJ/cm^2 UVB), twice a week for 15 weeks.

During the subsequent 20 weeks, the appearance of tumors was monitored weekly, the

lesions were mapped, counted, and their volumes determined. The number of tumors per

mouse (multiplicity) and the tumor burden are expressed as average values ± S.E.M. based on

the total number of animals at risk.

Figure 5. Pharmacological upregulation of Nrf2 in the skin of SKH-1 hairless mice protects against inflammation caused by solar-simulated UV radiation. Quantitative real-time PCR analysis of mRNA of IL-6 (**A,D,G**), IL-1β (**B**,**E,H**) and COX-2 (**C,F,I**) in skin samples of non-irradiated WT SKH-1 hairless mice (**A-C**), or WT (**D-F**) and Nrf2-KO (**G-I**) animals 24 h after acute exposure to a single dose (UVB component = 400 mJ/cm^2) of solar-simulated UV radiation. Two groups of each genotype of mice (n=5) were used. The first one was treated with vehicle (80% acetone), whereas the second one received TBE-31 (three daily doses of 40 nmol per mouse, every 24 h, applied topically). Data were normalized with respect to levels in vehicle-treated non-irradiated skin. Results are means ± S.D. *, $p < 0.05$ for comparison between irradiated vehicle-treated and irradiated TBE-31-treated animals.

Figure 6. Pharmacological upregulation of Nrf2 by TBE-31 protects against cutaneous carcinogenesis mediated by solar-simulated UV radiation in mice receiving azathioprine therapy. WT SKH-1 hairless mice (n=30) were treated with azathioprine (1 mg/kg/day, orally, dissolved in the drinking water), and either vehicle (80% acetone) or TBE-31 (40 nmol per mouse, twice a week, topically, in 200 μl of 80% acetone). Two weeks after beginning of treatment with azathioprine and TBE-31, the animals were exposed chronically to solar-simulated UV radiation (comprised of 2 J/cm^2 UVA and 90 mJ/cm^2 UVB), twice a week for a further 15 weeks. Irradiation was then stopped, but treatment with both azathioprine and TBE-31 was continued for the duration of the experiment. During the subsequent 16 weeks, the appearance of tumors was monitored weekly, the lesions were mapped, counted, and their volumes determined. The graphs show tumor incidence (**A**), multiplicity (**B**) and burden (**C**). The number of tumors per mouse (multiplicity) and the tumor volume are expressed as average values ± S.E.M. based on the total number of animals at risk.

30

Figure 7. Topical application of extracts containing the Nrf2 activator sulforaphane reduces the degree of skin erythema following acute exposure to solar-simulated UV radiation in healthy human subjects. (**A**) Study design. Twenty-four healthy human subjects received topically, on their upper back, two types of plant extracts: sulforaphane-rich (SF, active), and glucoraphanin-rich (GR, placebo), 3 times, 24 h apart. One day after the last extract application, small areas (approximately 1 cm^2) of skin were exposed to a range of doses of solar simulated UV radiation. Erythema was determined 24 h later semi-quantitatively by naked eye and quantified objectively using an erythema meter. (**B**) Sum of erythema for all doses of solar simulated UV radiation. Data are presented as the average of 3 independent measurements for the irradiated sites minus the average of 3 measurements for non-irradiated (background) sites. The difference between placebo- and active extract-treated sites is statistically significant ($p = 0.02$).
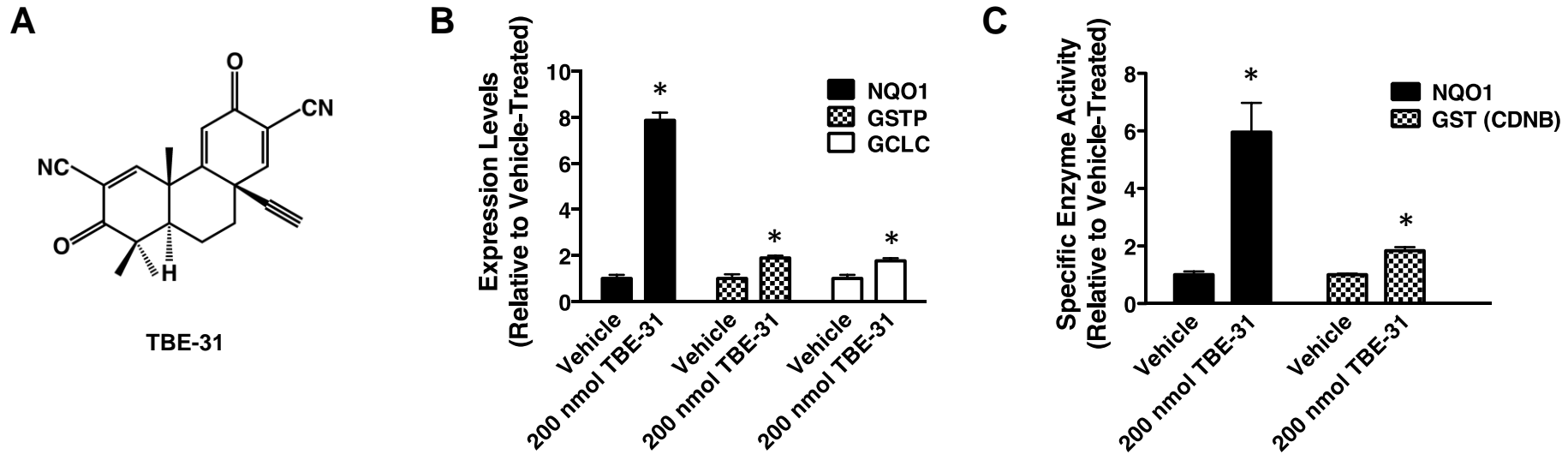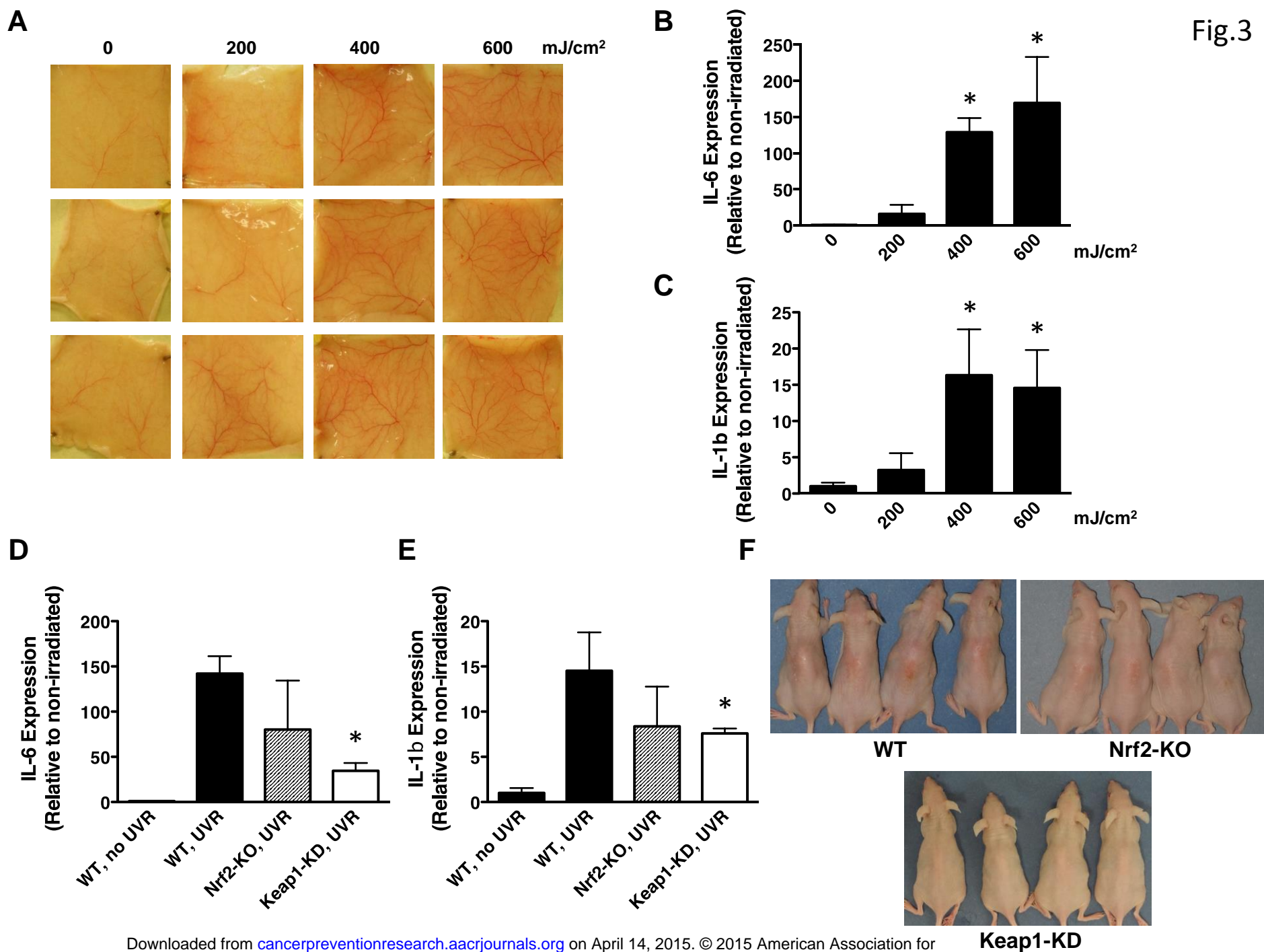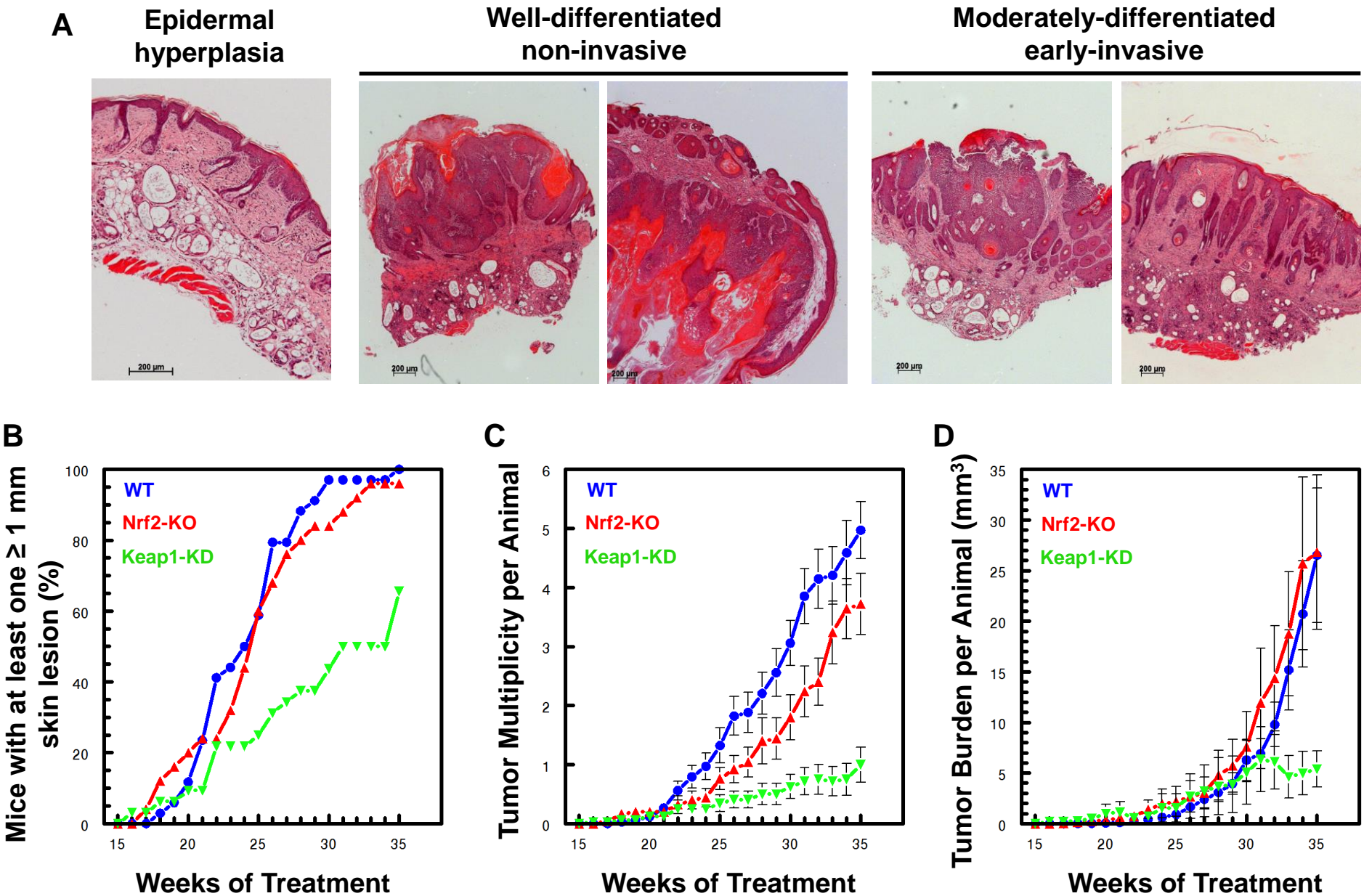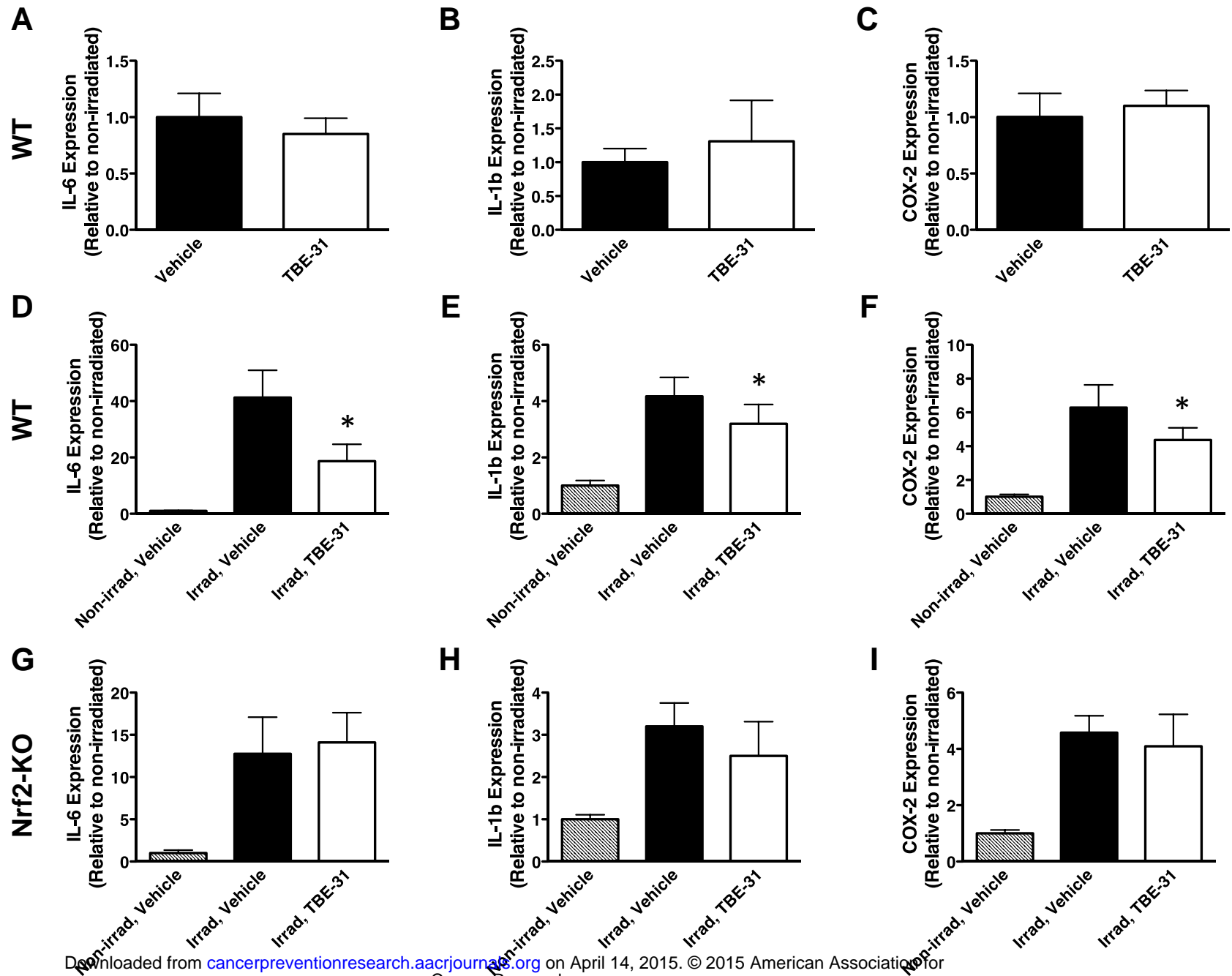
Fig.1

A

B

C

D

E

F

Fig.2

A

TBE-31

B

C

A

0   200   400   600   mJ/cm²

B

IL-6 Expression (Relative to non-irradiated)

250
200
150
100
50
0

*   *

0   200   400   600   mJ/cm²

C

IL-1b Expression (Relative to non-irradiated)

25
20
15
10
5
0

*   *

0   200   400   600   mJ/cm²

D

IL-6 Expression (Relative to non-irradiated)

200
150
100
50
0

*

WT, no UVR   WT, UVR   Nrf2-KO, UVR   Keap1-KD, UVR

E

IL-1b Expression (Relative to non-irradiated)

20
15
10
5
0

*

WT, no UVR   WT, UVR   Nrf2-KO, UVR   Keap1-KD, UVR

F

WT   Nrf2-KO

Keap1-KD

Fig.3

Fig.4

A

Epidermal hyperplasia

Well-differentiated non-invasive

Moderately-differentiated early-invasive

B

Mice with at least one ≥ 1 mm skin lesion (%)

WT
Nrf2-KO
Keap1-KD

Weeks of Treatment

C

Tumor Multiplicity per Animal

WT
Nrf2-KO
Keap1-KD

Weeks of Treatment

D

Tumor Burden per Animal (mm^3)

WT
Nrf2-KO
Keap1-KD

Weeks of Treatment

Fig.5

Fig.6

A

B

C

Fig.7

AAGR American Association for Cancer Research
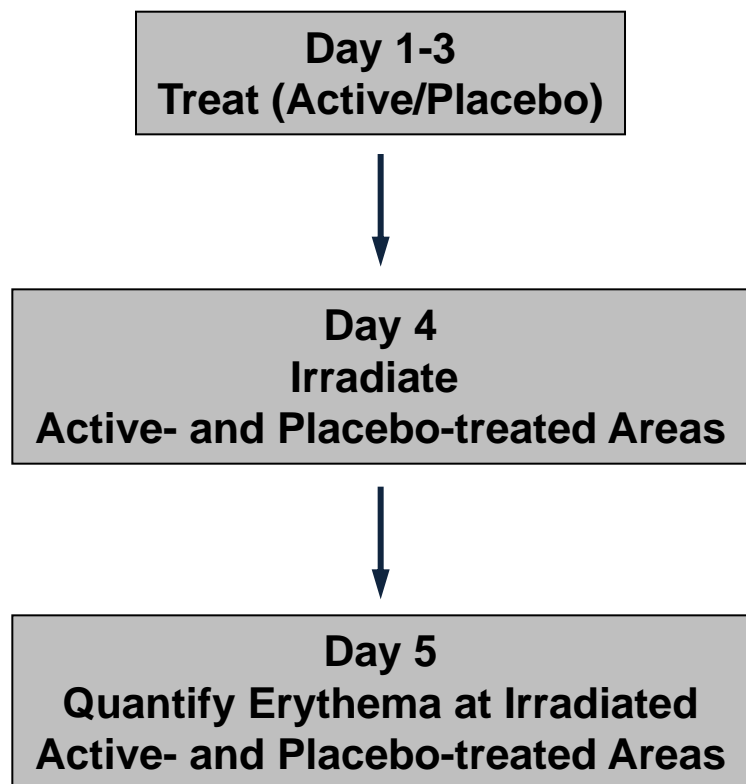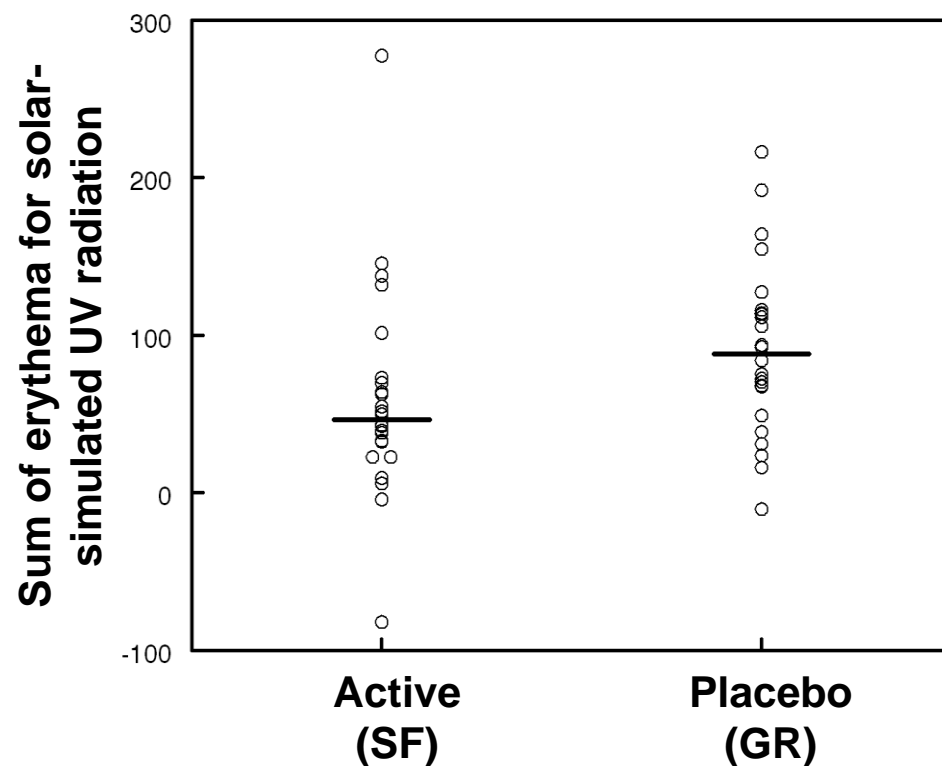
Cancer Prevention Research

Nrf2 activation protects against solar-simulated ultraviolet radiation in mice and humans

Elena V. Knatko, Sally H. Ibbotson, Ying Zhang, et al.

Updated version	Access the most recent version of this article at: doi:10.1158/1940-6207.CAPR-14-0362
Supplementary Material	Access the most recent supplemental material at: http://cancerpreventionresearch.aacrjournals.org/content/suppl/2015/03/25/1940-6207.CAPR-14-0362.DC1.html
Author Manuscript	Author manuscripts have been peer reviewed and accepted for publication but have not yet been edited.

E-mail alerts	Sign up to receive free email-alerts related to this article or journal.
Reprints and Subscriptions	To order reprints of this article or to subscribe to the journal, contact the AACR Publications Department at pubs@aacr.org.
Permissions	To request permission to re-use all or part of this article, contact the AACR Publications Department at permissions@aacr.org.